
Binding of a Diphosphorylated-ITAM Peptide to Spleen Tyrosine Kinase (Syk) Induces Distal Conformational Changes: A Hydrogen Exchange Mass Spectrometry Study

M. Isabel Catalina

Department of Biomolecular Mass Spectrometry, Utrecht Institute for Pharmaceutical Sciences (UIPS) and Bijvoet Center for Biomolecular Research, Utrecht University, Utrecht, The Netherlands

Marcel J. E. Fischer, Frank J. Dekker,* and Rob M. J. Liskamp

Department of Medicinal Chemistry, Utrecht Institute for Pharmaceutical Sciences (UIPS), Utrecht University, Utrecht, The Netherlands

Albert J. R. Heck

Department of Biomolecular Mass Spectrometry, Utrecht Institute for Pharmaceutical Sciences (UIPS) and Bijvoet Center for Biomolecular Research, Utrecht University, Utrecht, The Netherlands

Structural flexibility plays a crucial role in protein function. To assess whether specific structural changes are associated with the binding of an immunoreceptor tyrosine-based activation motif (ITAM) to the tandem Src homology-2 domains (tSH2) of the spleen tyrosine kinase [EC 2.7.7.112] (Syk), we used an approach based on protein hydrogen/deuterium exchange in the presence and absence of the diphosphorylated ITAM peptide. The protein deuterium uptake by the intact Syk protein was monitored in time by electrospray mass spectrometry, which revealed a dramatic relative decrease in deuterium uptake when the protein was bound to the ITAM peptide, suggesting an overall change in protein dynamics. Subsequently, the deuterium incorporation of individual segments of the protein was investigated using proteolysis and matrix-assisted laser desorption ionization time-of-flight (MALDI-TOF) peptide mass-analysis, which revealed that several regions of Syk tSH2 are significantly more protected from exchange in the presence of the ITAM peptide. Four protected regions encompass the phosphotyrosine and hydrophobic binding sites on the SH2 domains, whereas two other protected regions are located in the inter-SH2 linker motif and do not make any direct contacts with the peptide. Interestingly, our data suggest that binding of the ITAM peptide to Syk tSH2 induces distal structural effects on the protein that stabilize the inter-SH2 linker region, possibly by raising the degree of helical structure upon binding. (J Am Soc Mass Spectrom 2005, 16, 1039–1051) © 2005 American Society for Mass Spectrometry

Substrate recognition and allosteric regulation are vital events in cell signaling. In these processes, protein flexibility plays a key role. Proteins are assumed to exist in a number of energetically similar conformations. Under this assumption, a ligand will selectively bind the best fitting conformer(s). The study of the structural mobility of a protein in its free (unbound) state is challenging, as experimental structure determinations of flexible parts of a protein are often ambiguous. Here, the impact of ligand binding on the structural flexibility of the tandem SH2 domains of the

Syk protein kinase is investigated using hydrogen/deuterium exchange in combination with mass spectrometry.

The Syk family of nonreceptor protein-tyrosine kinases (PTKs) comprises two known members, Zap-70 and Syk. Syk is a 72-kDa cytoplasmic protein that has been implicated in a variety of hematopoietic cell responses, in particular immunoreceptor-signaling events that mediate diverse cellular responses as proliferation, differentiation, and phagocytosis [1]. Syk was also shown to be functionally important in nonhematopoietic cells like fibroblasts, epithelial cells, breast tissue, hepatocytes, neural cells, and vascular endothelial cells [2].

The Syk family PTKs possess two Src homology-2 (SH2) domains positioned in tandem (tSH2) and located N-terminally to the kinase domain. These proteins are

Published online May 23, 2005

Address reprint requests to Dr. A. J. R. Heck, Department of Biomolecular Mass Spectrometry, Utrecht University, Sorbonnelaan 16, 3584 CA Utrecht, The Netherlands. E-mail: a.j.r.heck@chem.uu.nl

* Current address: Max Planck Institute for Molecular Physiology, Otto Hahn Strasse 11, 44227 Dortmund, Germany.

recruited to cell surface receptors through the interactions of their tandem SH2 domains with tyrosine-phosphorylated sequence motifs termed immunoreceptor tyrosine-based activation motifs (ITAMs) [3]. ITAMs have the consensus sequence $Y_{xx}(L/I)-x_{7/8}.Y_{xx}(L/I)$ [3]. Phosphorylation of both tyrosines residues within ITAM [diphosphorylated ITAM peptide (2pITAM)] by the Src-family PTKs [4] is required for binding of the Syk family kinases to the receptor subunits. This motif is present in the β and γ chains of Fc ϵ RI (IgE receptor), in the ξ subunit of the T-cell receptor complex, and in the immunoglobulins Ig β and Ig α of the B-cell receptor [5, 6]. In vitro, binding of Syk to the 2pITAM of Fc ϵ RI results in a conformational change in Syk, accompanied by an increase in its enzymatic activity [7, 8]. This suggests the functional importance of the tSH2 domain-mediated association of Syk with Fc ϵ RI [9]. The catalytic domain of Syk may be regulated by intramolecular interactions with its adjacent domains [10] and it has been suggested that Syk binding to phosphorylated γ subunits following Fc ϵ RI engagement in vivo stimulates Syk kinase activity, somewhat similar to the intramolecular interactions that regulate the catalytic ac-

tivity of the Src kinases [11–13]. The tandem SH2 domains of the Syk kinase (Syk tSH2) are able to recognize a variety of doubly phosphorylated ITAMs, varying considerably not only in sequence but also in the length of the region between the two phosphotyrosines [14–16]. Previous studies have shown that the inter-SH2 domain of the Syk family PTKs have a coiled-coil structure that may be involved in protein–protein interactions and the regulation of kinase activity [9].

The elucidation of the crystal structure of the tSH2 domain of Syk in complex with a 2pITAM derived from the CD3- ϵ chain of the T-cell receptor (ϵ -2pITAM) (Figure 1a) [17] gave the first structural hint on the substantial flexibility of the protein. Already six different copies of the bound protein were found in the asymmetric unit, and alignment of the different structures revealed remarkable flexibility in the relative orientation of the two SH2 domains. The latter may explain the ability of Syk to bind ITAMs differing in inter-motif sequence. The crystal structure of the ligand-free Syk tSH2 is not available to date, but the structure of the tSH2 domains of the family-related

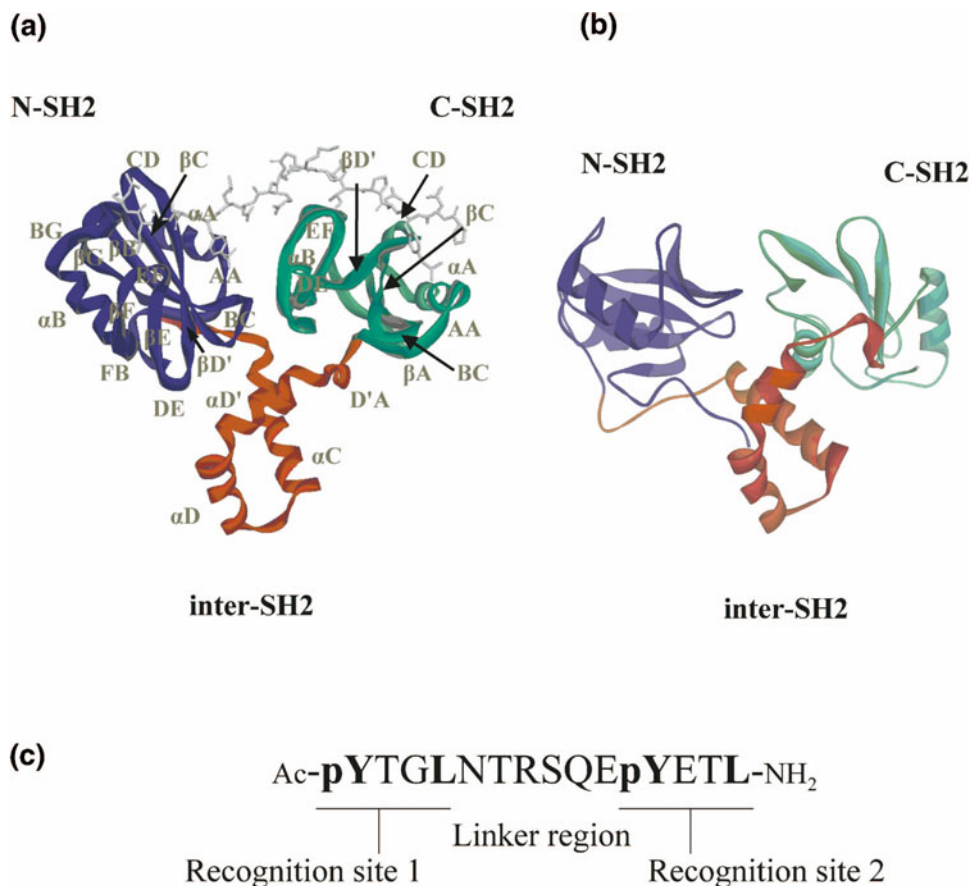


Figure 1. Ribbon diagrams of (a) the tandem SH2 domains of Syk in complex with ϵ -2pITAM and (b) Zap-70 in its ligand-free state. The N-SH2 domains are depicted in blue, the C-terminal SH2 in green, and the inter-SH2 linker region in red. The bound ITAM peptide ligand is shown in gray. Secondary structure elements are labeled according to the notation adopted in Figure 6. Protein data bank codes are 1A81 for the Syk tSH2 complex and 1M61 for the Zap-70 tSH2. (c) Amino acid sequence of the γ -2pITAM peptide used in our studies.

Zap-70 kinase has been revealed by X-ray crystallography, and its backbone dynamics has been studied by NMR (Figure 1b) [18]. Although Zap-70 and Syk do not share that much sequence homology (i.e., 55%) the overall topology of the Syk tSH2 domain is quite similar to the one in Zap-70 [17]. The obtained structures suggest that the two SH2 domains are able to undergo large inter-domain movements. No defined NMR signals could be detected for the two helices connecting the SH2 domains (Figure 1b), likely attributable to rapid conformational dynamics. Furthermore, isothermal calorimetry, stopped-flow kinetics of binding, and fluorescence spectroscopy experiments revealed that the enthalpy and the on-rate for binding of Syk tSH2 to ITAM peptides had an unusual nonlinear dependence on temperature. All these data could be well described by a model based on a conformational equilibrium between two conformers of Syk tSH2 in the unbound form, i.e., an open and a closed state [19]. Recently, Kumaran et al. [20] tested the two conformers hypothesis by locking the tSH2 domains with a disulfide bridge. Characterization of the binding thermodynamics of this mutant showed that it behaved as predicted for a closed conformer.

Here, we use a direct method to probe and characterize the flexibility of the Syk protein and the changes in protein mobility upon ITAM binding. Very low sample consumption and fast analysis give a readily structural overview on protein flexibility. The methodology is based on the solvent accessibility to the protein. We used two complementary approaches (Figure 2). First, hydrogen/deuterium exchange (HDX) on the intact Syk tSH2 (both, free and in complex) was monitored continuously by electrospray ionization mass spectrometry (ESI-MS) [21, 22], which provided a general view of the overall differences in solvent accessibility (and/or hydrogen bonding) of the free and ITAM-bound Syk protein. Second, HDX on the intact protein (both, free and ITAM-bound) followed by quenching at pH 2.4 (0 °C), proteolysis with pepsin, and subsequent peptide mass analysis by MALDI-MS [23, 24] was performed in order to localize the structural changes in specific regions of Syk tSH2 upon ITAM binding.

Our data reveal that binding of the tSH2 domain of Syk to the 2pITAM peptide derived from the FcεRI γ chain (γ-2pITAM) leads to a major change in overall protein solvent accessibility. As expected, the SH2 domains–ITAM interaction region displayed a decrease in solvent accessibility upon ITAM binding. More interestingly, the inter-SH2 domain linker region turned out to be highly solvent accessible in the ligand-free Syk, whereas a dramatic decrease in solvent accessibility occurred upon ITAM binding. The high degree of freedom in the relative position of the SH2 domains in the ligand-free Syk provides the possibility to accommodate ITAM motifs with different spacer regions. The latter is crucial for their function in the different types of cells where Syk is present. The observed conformational

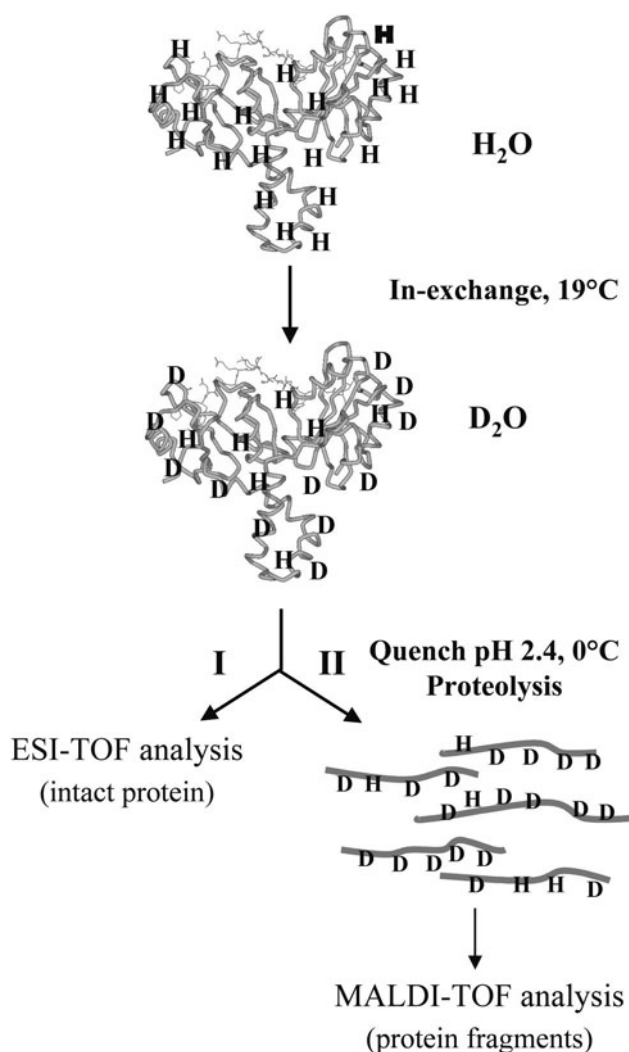


Figure 2. Scheme of the two-pronged approach used in this study. Syk tSH2 is incubated with or without γ -2pITAM peptide in D₂O at 19 °C. In Approach I, the increase in mass of the intact protein through deuterium incorporation is continuously monitored by ESI-MS. In Approach II, at a number of time points the labeling reaction is quenched by lowering the pH to 2.4 at 0 °C, the protein is pepsin digested, and the deuterium uptake in the protein fragments are mass analyzed by MALDI-TOF.

stabilization of the inter-domains region upon ligand binding and the related reduction in freedom of movement of the SH2 domains are likely one of the main signaling events activating the kinase domain.

Experimental

Materials

Ultrafree-0.5 centrifugal filter devices for buffer exchange were obtained from Millipore (Billerica, MA). D₂O (99.9% deuterium) packed in 0.7-ml ampoules was purchased from Sigma-Aldrich (Zwijndrecht, The Netherlands). Pepsin immobilized on cross-linked 6% beaded agarose was obtained from Pierce (Cheshire, UK). α -Cyano-4-hydroxycinnamic acid, succinic acid,

citric acid, nitrocellulose (70% solution in isopropanol), and ammonium acetate were purchased from Sigma-Aldrich. Acetone (proanalysis grade) was obtained from Merck (Darmstadt, Germany). The 2pITAM peptide derived from the Fc ϵ RI γ chain, Ac-pYTGLNTR-SQEpYETL-NH₂ (monoisotopic mass 1975.7966 Da), was synthesized using Fmoc [N-(9-fluorenyl)methoxycarbonyl] chemistry and purified by C-18 reverse phase HPLC as described previously [15,25].

Protein Preparation

Fusion clones of the glutathione S-transferase (GST) Syk tSH2 domain were kindly provided by Dr. S. Kumaran, Washington University, St. Louis, MO. The *Escherichia coli* strain BL21 contained the pGEX-KT vector with amino acids 10-273 of human Syk, enabling thrombin cleavage of the GST moiety. Isolation procedures were generally as previously described [26]. The collected cellular protein fraction was purified on a GSTrap column (Amersham Pharmacia Biotech, Freiburg, Germany). On-column cleavage with thrombin resulted in pure (>98%) Syk tSH2, as determined from mass spectral analysis and SDS-PAGE. The protein concentration was determined by UV using a molar extinction coefficient of 31,630 at 280 nm.

Global H/D Exchange in Syk tSH2 Monitored by ESI-MS (Approach I, Figure 2)

100- μ M samples of either ligand-free Syk tSH2 or protein bound to the γ -2pITAM peptide (protein mixed with a 3-times peptide excess), were diluted 20 times with 65 mM ammonium acetate in D₂O (equivalent to neutral pH) to give a final percentage of D₂O of 95%. Mass spectrometric measurements were performed with an LCT-TOF mass spectrometer (Micromass Manchester, UK) equipped with a Z-electrospray source. Protein solutions, typically 100 μ L, were infused into the LCT mass spectrometer at 2 μ L/min using a Harvard syringe pump (Holliston, MA). The ionization chamber of the mass spectrometer was flushed with D₂O for a few minutes prior to analysis. Electrospray was obtained with a capillary voltage of 2500 V. For mass calibration, an aqueous CsI solution was used at a concentration of 2 mg/ml in a 50% isopropanol solution. Typical ESI-MS spectra of the noncovalent protein-peptide complex would show exclusively the multiply charged ions corresponding to the molecular mass of the noncovalent Syk-ITAM complex. To analyze the deuterium incorporation in the protein, high cone voltages of 190 V were used to disrupt the protein-peptide complex, providing the fragment ions of the intact protein and the ligand. The same cone voltage of 190 V was applied when spraying the ligand-free protein to maintain the same experimental conditions. The total number of exchangeable hydrogens of Syk tSH2 was calculated from its amino acid sequence, being 465.5 in

95% D₂O out of a total of 490. Protein masses were determined by ESI-MS; the combined data from several charge states of the protein in each spectrum were used to calculate the molecular mass.

To determine the molecular mass of the nondeuterated protein, 5 μ M protein solutions in 50% acetonitrile/1% formic acid were analyzed. The experimental molecular mass of the Syk tSH2 domain was 29,788 (\pm 1) Da, in agreement with the calculated mass of 29,787.95 Da.

H/D Exchange in Syk tSH2 Followed by Quenching, Pepsin Digestion, and MALDI-MS (Approach II, Figure 2)

Ten microliters of a 200 μ M Syk tSH2 solution in 150 mM aqueous ammonium acetate were 10-times diluted with D₂O (equivalent to neutral pH), to give a final percentage for D₂O of 90%. The solutions were incubated at 19 °C. After a preassigned period of time ranging from 0 to 30 min, 10 μ L aliquots were taken from the deuterated protein solution and mixed with 100 μ L of ice-cold quench solution and 30 μ L of pepsin bead slurry (previously washed 4 times with 0.450 ml quench buffer). The quench solution consisted of 25 mM citric acid and 25 mM succinic acid (pH 2.4) [27]. This brought the pH of the Syk tSH2 solution down to 2.4 and quenched the H/D exchange [28]. The mixture was incubated on ice with occasional mixing for 7 min. Next, the mixture was centrifuged for 20 s at 13,000 *g* at 4 °C, to remove the pepsin beads. The supernatant was collected and immediately frozen in liquid N₂. Samples were stored at -80 °C until MALDI-MS analysis. The samples of the Syk tSH2 bound to the γ -2pITAM peptide were prepared in the same way. Two different series of experiments wherein the concentration of the γ -2pITAM peptide was either 3- or 7-fold the concentration of the Syk tSH2 protein were performed. For each protein:peptide ratio, experiments were repeated at least twice. They all showed similar qualitative results for deuterium incorporation in each of the protein fragments. The data presented in the figures originate from one such an incubation experiment at a protein:peptide ratio of 1:7.

In- and back-exchange controls were performed as follows: in-exchange of deuterium under quench conditions was measured by adding the protein solution directly to a mix of D₂O, quench solution, and pepsin (this corresponds to time zero). Then, the same procedure was followed as described above. Back-exchange controls were measured by incubating the protein in a D₂O solution with 1% formic acid overnight at 20 °C and thereafter at 50 °C for 15 min to achieve complete exchange. In order to determine the amount of label lost during sample workup (back-exchange), a control sample was fully deuterated, quenched, pepsin digested, and analyzed by MALDI-MS. MALDI-MS analysis was performed with a MALDI TOF-TOF instrument (Ap-

plied Biosystems 4700 Proteomics analyzer, Framingham, MA) in the reflectron mode. Data were acquired at a 200 Hz laser repetition rate, a 20 kV accelerating voltage, a 70% grid voltage, and a digitizer bin size of 0.5 ns. Samples were prepared using the thin-layer preparation technique as described previously [27,29]. Briefly, 0.8 μl of an acetone solution saturated in α -cyano-4-hydroxycinnamic acid and 2 mg/ml nitrocellulose containing a mass calibration mixture (1 pmol/ μl of each calibration compound) was spotted onto the MALDI sample target generating a thin-layer spot. Subsequently, the target was cooled down to -20°C . The mass calibration mixture consisted of the following compounds (in brackets the monoisotopic masses of the singly protonated species in Da): des-arg¹-bradykinin (904.4681), angiotensin I (1296.6853), Glu¹-fibrinopeptide B (1570.6774), and ACTH 18-39 (2465.1989). The deuterated samples were thawed rapidly, 0.8 μl spotted on the thin-layer, and dried under a nitrogen gas stream. Immediately after crystallization, the MALDI plate was transferred into the vacuum chamber of the mass spectrometer. Each protein solution, corresponding to one data point, was spotted in three different places and two spectra per spot were acquired. Each spectrum was the average of approximately 3000 shots. The mass of each peptide was averaged over at least three spectra.

Data analysis was performed with the Data Explorer software version 4.5 (Applied Biosystems). Spectra were calibrated with the above-mentioned peptides and centroids of each peak were determined. The number of deuteriums in-exchanged at a time t , $D(t)$, was calculated using the following equation [30,31].

$$D(t) = \frac{m(t) - m(0)}{m(100) - m(0)} \times N \quad (1)$$

where $m(t)$ and $m(0)$ are the observed centroid mass of a peptide at time point t and zero (in-exchange control), respectively; and $m(100)$ is the observed mass of a fully exchanged peptide (back-exchange control). N is the total number of peptide amide protons in the peptide.

Results

H/D exchange reactions are highly sensitive to changes in structure and dynamics accompanying protein folding, ligand binding, and protein-protein interactions [32–36]. In the case of the 29-kDa Syk tSH2, we monitored: (1) deuterium incorporation in the intact protein, and (2) deuterium incorporation in specific protein segments. Whereas the aim in the first approach is to readily obtain an idea of the dimension of possible structural changes induced upon γ -2pITAM binding, in the second approach, kinetics of structural changes at a medium level of structural resolution are obtained.

H/D Exchange of Intact Syk tSH2 Monitored by ESI-MS

Typical electrospray ionization mass spectra of the deuterated Syk tSH2, either ligand-free or bound to γ -2pITAM, are shown in Figure 3a and b. The spectra of ligand-free Syk tSH2 present a bimodal charge envelope: the most abundant charge envelope is centered at the 12-fold protonated protein ion, whereas the less intense envelope is localized around the 16+ protein ion (Figure 3a). In contrast, the ESI spectra of the Syk- γ -2pITAM complex show a single charge envelope distribution with only two markedly intense protein ions, namely the 13+ and 12+. Molecular masses of nondeuterated Syk tSH2 and Syk tSH2- γ -2pITAM complex were measured to be 29,788 (± 1) and 31,765 (± 2) Da, respectively, in agreement with the calculated masses from the amino acid sequences.

The HDX kinetics of the ligand-free and γ -2pITAM-bound Syk tSH2 was followed by incubating each in a 65 mM ammonium acetate D_2O solution (equivalent to neutral pD) and continuously monitoring the increase of the protein mass in the ESI mass spectra. The total number of exchangeable hydrogens in the protein is 490, as calculated from its amino acid sequence. The noncovalent complex of Syk tSH2 with γ -2pITAM is easily preserved in the gas phase of the mass spectrometer as revealed by the spectrum shown in Figure 3b. However, to measure the deuterium uptake in the protein, the noncovalent complex was dissociated in the gas phase by applying a high cone voltage in the source interface. This higher cone voltage resulted in ESI mass spectra as shown in Figure 3c, whereby we monitored the mass of the so-released protein. The measured difference in mass between the Syk- γ -2pITAM and free Syk protein was 2011 ± 2 Da, indicating that the ITAM peptide is nearly fully H/D exchanged. In the insets of Figure 3a and c, the shift in m/z of the 12+ protein ions after 15 min of incubation in aqueous (D_2O) ammonium acetate in the absence (Figure 3a) and presence (Figure 3c) of ligand is shown. The Syk protein in the Syk- γ -2pITAM complex is observed at lower m/z due to lower deuterium incorporation than in the ligand-free Syk protein.

The protein deuterium uptake in time is displayed in Figure 4. The deuterium incorporation appears to be very rapid: within 1 min over 80% of the available protons have been exchanged in the ligand-free protein and some 72% in the ligand-bound protein. From the curves, it is apparent that ligand binding has a remarkable effect on deuterium incorporation, overall diminishing it quite dramatically.

H/D Exchange in Specific Segments of Syk tSH2

Enzymatical digestion of a protein after a designated incubation time in D_2O allows the study of its structure and dynamics changes at medium level of structural resolution [32,37–39]. The Syk tSH2, with or without

the ITAM peptide, was incubated in D₂O up to 25 min. After a series of time periods, the exchange was quenched at pH 2.4 (0 °C) and the protein digested with pepsin.

The γ -2pITAM concentration was 7-fold the Syk protein concentration, assuring more than 99% Syk tSH2- γ -2pITAM complex at all times (the complex dissociation constant is approximately 40 nM) [40], which ensures that H/D exchange does not out-compete the ligand binding reaction [36].

The peptide fragments obtained after pepsin digestion were analyzed by MALDI-MS (Figure 5a) and could be assigned to particular segments of Syk tSH2 (Figure 6) by tandem MS. The observed peptides almost cover the full primary sequence of the protein (98%). Peak broadening because of deuterium incorporation (Figure 5b) lowers the signal-to-noise ratio. The latter, together with overlapping of peptide peaks, lead to exclusion of some peptides for further analysis. Therefore, only a subset of the peptides covering some 75% of the amino acid sequence was used for further analysis.

The average mass of each peptide was obtained by calculating the centroid of the full envelope of the isotopic peaks [24] with the aid of the DataExplorer software provided with the instrument. From the measured masses, the number of incorporated deuteriums was determined using eq 1 (for details see the Materials and Methods section). Controls for deuterium in-exchange and back-exchange were performed. The controls showed 8 to 12% in-exchange and about 40% back-exchange. These numbers were used to correct the H/D exchange data. The deuterium incorporation after specified time points [$D(t)$] in a peptide fragment were plotted versus time. Some typical examples for selected fragments are shown in Figure 7, comparing the exchange observed when Syk was ligand-free in solution with Syk when it was ITAM-bound. A substantial

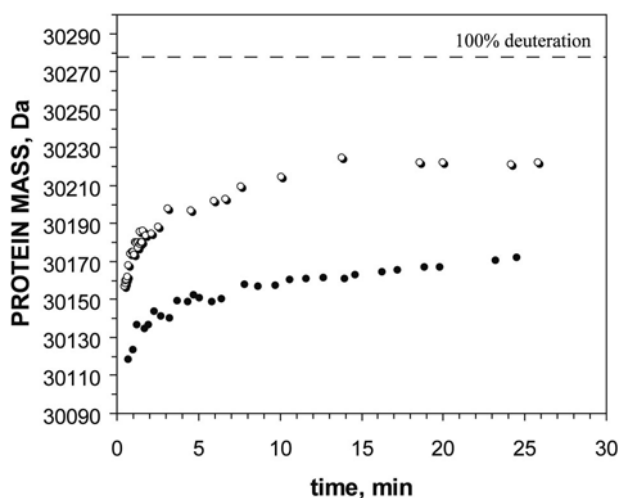


Figure 4. Kinetics of H/D exchange for Syk tSH2. The protein was exposed to buffered D₂O, as peptide ligand-free protein (open circles) and in complex with γ -2pITAM peptide (filled circles). The mass deviation errors fall within ± 3 Da.

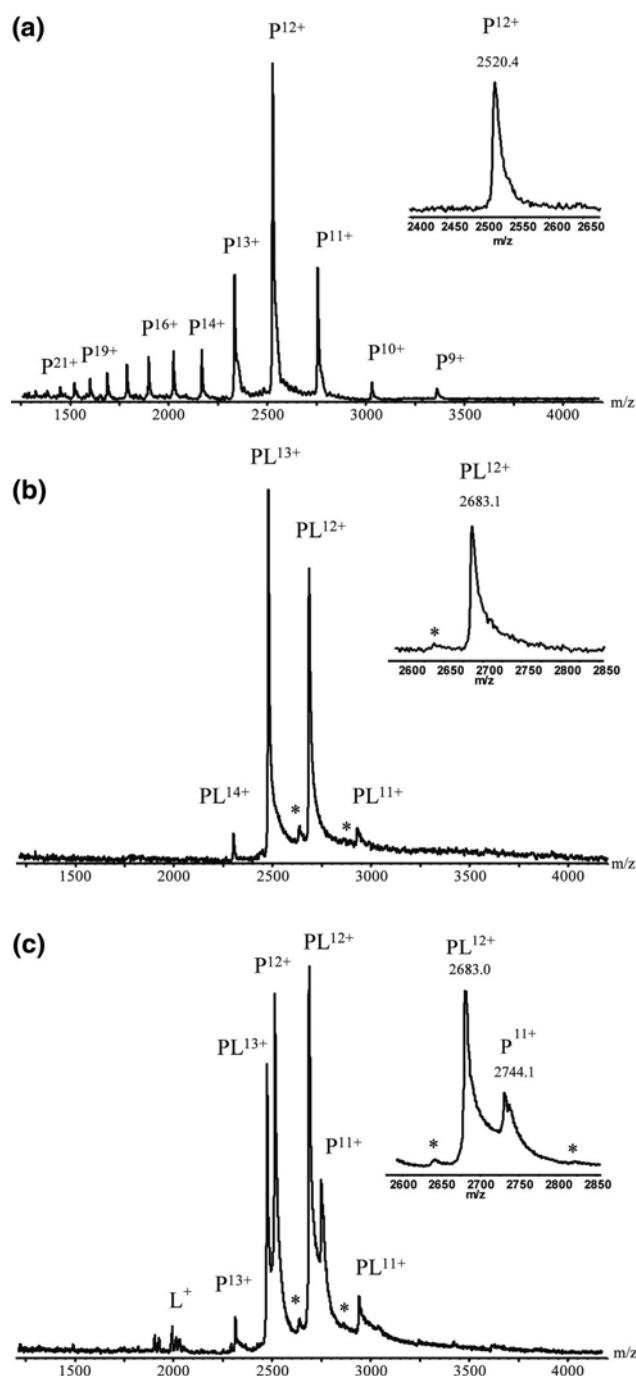


Figure 3. ESI-MS spectra of Syk tSH2 in a 95% D₂O solution containing ammonium acetate at a concentration of 65 mM (neutral pD) after 25 min incubation: (a) as ligand-free protein, (b) in complex with the γ -2pITAM at a cone voltage of 90 V; and (c) identical conditions as in (b) but the Syk- γ -2pITAM complex is partially dissociated by applying a higher cone voltage (CV, 190 V). P stands for protein, L for the ITAM peptide ligand and PL for the protein-peptide ligand complex. In superscript the number of charges of the ions is indicated. The asterisks annotate small ion signals representing protein ions bound to two ligands.

number of peptides showed a decrease in D -exchange following ITAM binding (Table 1), whereas others remained nearly unaltered. The amide hydrogens

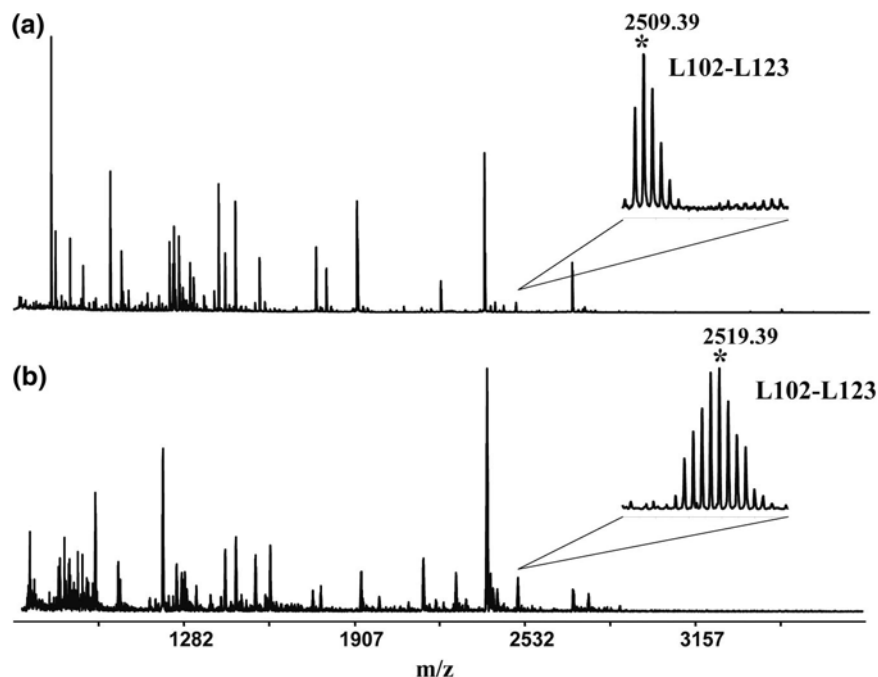


Figure 5. MALDI-TOF mass spectra of the pepsin digest of Syk tSH2. The upper spectrum (a) shows a pepsin digest of ligand-free Syk tSH2 in H_2O , and (b) in D_2O .

within peptides covering residues Y39-F51 and V132-L148 are clearly protected from HDX in the presence of γ -2pITAM (Figure 7a, b, Table 1). In contrast, the peptides covering F51-Y74 (Figure 7d, Table 1) and L205-F234 (Table 1) are largely unaffected by γ -2pITAM binding. Multiple peptides probing segments of both SH2 domains as well as the inter-domain region displayed significant variation in solvent accessibility in the presence of the bivalent peptide. Results for all analyzed protein fragments are summarized in Table 1. Given the experimental error [approximately ± 0.2 Da, as derived from the fittings of the kinetic curves (Figure 7)], we termed a protein fragment as protected when the mass difference of the H/D exchange protein fragment was ≥ 1 between the ligand-free and ligand-bound Syk tSH2 after 25 min of exchange.

Discussion

In this report, we have used H/D exchange in combination with mass spectrometry to study the effect of γ -2pITAM ligand binding to Syk. Locking the relative position of the Syk tandem SH2 domains through ITAM binding induces structural stabilizing effects that may influence the regulation of the Syk kinase enzymatic activity [9, 10]. Probing structural dynamics in proteins with hydrogen/deuterium exchange was introduced some five decades ago [41]. H/D exchange coupled with NMR provides detailed site-specific information on conformational changes induced by protein or ligand binding. Yet, structural flexibility within unbound state(s) of proteins is often inaccessible by these NMR-based approaches [18, 20]. In contrast, H/D exchange

coupled with mass spectrometry is sensitive for just these effects and provides increased sensitivity and the ability to analyze large proteins and protein complexes, although at the cost of reduced structural resolution [42].

Anderegg and Wagner [21] were among the first to report on how overall changes in protein conformational stability upon binding could be monitored by HDX in combination with electrospray ionization mass spectrometry. They probed the overall changes in solvent accessibility of the Src SH2 domain upon binding to several phosphorylated peptides and proposed that changes in deuterium incorporation upon binding could be rationalized in two ways [21]: First, ligand binding reduces deuterium uptake by shielding exchangeable hydrogens from the solvent. Second, reduced uptake is the result of changes in overall dynamics of the protein in the complex. It was argued that shielding of the protein surface by a small ligand would only represent a modest effect on HDX and, therefore, the major contribution in solvent protection upon binding would be accounted for by a change in protein structural dynamics. Since their study, comparable effects have been reported for other SH2 domains such as the ones of Hck and Grb2 [26, 43]. These MS-based findings are in agreement with several NMR studies that also revealed that ligand binding reduces the dynamics in quite a few different proteins containing SH2 domains [44–46].

In our study, we find that the deuterium uptake of Syk tSH2 when bound to the γ -2pITAM peptide is approximately 50 lower than when in its ligand-free state (Figure 4). In this approach, the deuteration of the

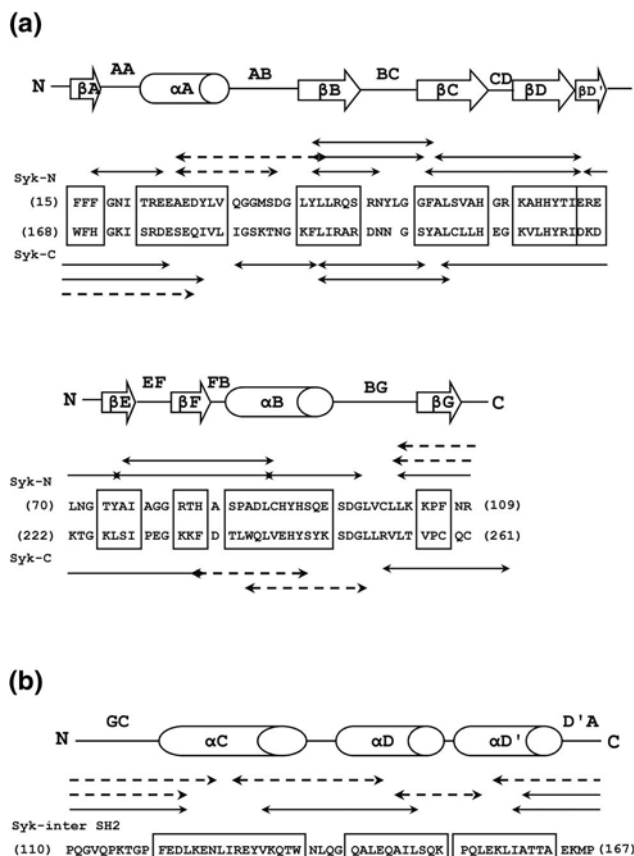


Figure 6. Syk tSH2 domain sequence and definition of the segments notation. (a) Alignment of the sequence of the N- and C-terminal SH2 domains of Syk tSH2, and (b) sequence of the inter-SH2 domain of Syk, based on the secondary structure definitions used by Fütterer et al. [17]. The arrows show the Syk tSH2 peptide fragments identified in the pepsin digest; dashed arrows show identified peptides that were not used for analysis because of their poor signal-to-noise ratio or overlap with other ion signals.

exchangeable side-chain and backbone hydrogens is followed. We propose two possible processes that may cause these large differences. First, the two SH2 domains may be held closer to each other and, as a result, the two SH2 domains might come in sufficient proximity to create an SH2–SH2 interface, which is then shielded from the solvent. Second, upon ligand binding, significant changes in structural dynamics may occur. The hypothesis of an SH2–SH2 interface generated upon binding to ITAM is to some extent supported by the crystal structure of Syk tSH2 in complex with ε -2pITAM [17]. Fütterer et al. described structural regions of the Syk N-SH2 that came into contact with the Syk C-SH2 upon binding [17]. Regarding possible changes in structural dynamics, it has been suggested that the inter SH2-domain linker might undergo a remarkable structural change upon binding, as it is a key player in the relative orientation of the two SH2 domains. It may be argued that the mobility of Syk would get dramatically restrained upon the bivalent peptide binding [17,19,20]. Supporting the global H/D

exchange results, we also observed a change in charge-state distribution upon ligand binding (Figure 3a,b), which indicates a reduction of the overall protein dynamics upon binding [33,47–49].

As these data suggested that protein dynamics might change upon binding of Syk tSH2 to γ -2pITAM, we headed to localize such changes at more structural detail. By enzymatically digesting the Syk protein after a designated incubation time in D_2O , the changes in backbone dynamics at a medium level of structural resolution could be followed. We applied this methodology to understand the nature of conformational changes in solution in the ligand-free Syk tSH2 (where no structural data are available to date) of Syk kinase. By following the mass of the protein fragments as a function of incubation time in D_2O , we could identify regions of Syk that are either sensitive or insensitive to γ -2pITAM binding (Table 1, e.g., Figure 7a,d). The results were evaluated in the context of the crystal structure of the Syk tSH2 (Figure 8). Several regions showed similar H/D exchange behavior independent of the presence or absence of γ -2pITAM. Several other regions displayed exchange protection in the presence of γ -2pITAM. In particular regions F17–E23, Y39–F51, and Y74–L88 in the Syk N-SH2 domain; region L193–L205 in the Syk C-SH2 domain; and regions L103–L123, V132–L148, I158–I181 covering about 75% of the inter-SH2 domain linker region, were protected from exchange. Thus, not only regions in the binding sites, but also distal to them, were affected. We will now discuss the effects upon ITAM binding on these regions in more detail.

The Inter-SH2 Linker Region

Each SH2 domain of Syk contains binding pockets that selectively bind to the ITAM peptide. In contrast, the inter-SH2 linker region has no direct contacts with the ITAM peptide and therefore, differences in deuterium uptake upon binding can only be explained by changes in structural dynamics. Four peptides encompassing 75% of the SH2-linker amino acid sequences are found to be significantly protected upon binding. The region I158–F192 is defined by peptides I158–E176 and A159–I181 (Table 1), which show a protection of two exchangeable hydrogens. The latter region is extended along the inter-SH2 motif and the Syk C-SH2 domain, embracing the C-terminal end of the α D' helix, the D'A loop, β A sheet, the AA loop, and the N-terminal end of the α A helix (Figure 6). At the α A helix, arginine 175 (α A2) participates in the phosphotyrosine-binding site (see below), and, therefore, the origin of the decreased deuterium incorporation upon binding in this region could be attributed to either direct phosphorylated tyrosine (pY) binding or change in structural dynamics. In contrast, two other peptides in the SH2-linker region are not directly involved in the protein–peptide interface but undergo a significant deuterium protection along the inter-SH2 linker region. These peptides are L103–L123 and V132–

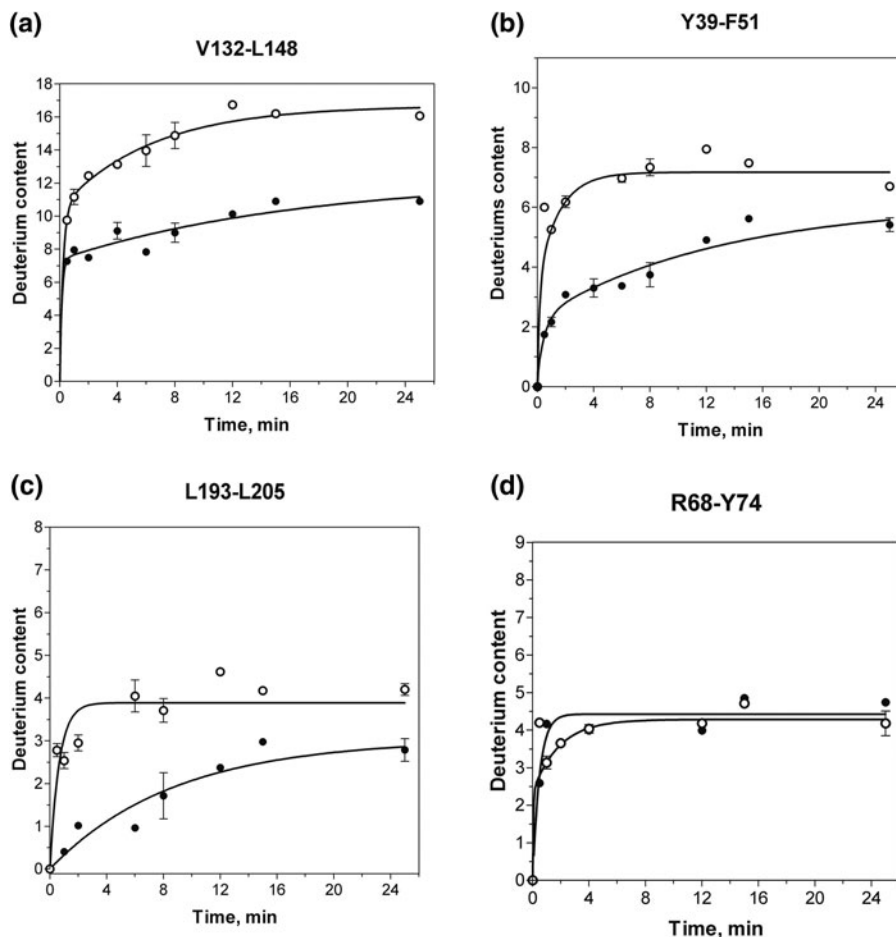


Figure 7. Kinetics of H/D exchange for selected peptide fragments. Deuterium up-take is plotted against the incubation time in D_2O at pH 6.8 in the absence (open circles) and presence (filled circles) of γ -2pITAM for peptides corresponding to residues V132-L149 (a), Y39-F51 (b), L193-L205 (c), and R68-Y74 (d) in Syk. The data in the panels are fitted to single or double exponentials for visualization purposes only.

L148. The peptide fragment L103-L123 partly shares its amino acid sequence with the Syk N-SH2; yet, in this region, no direct involvement in the protein-peptide interface is observed, and therefore, exchange protection can only be explained through changes in dynamics. Peptide V132-L148 (Figure 7a) is embedded in the middle of the SH2-linker region. This protein fragment undergoes a remarkable exchange protection upon γ -2pITAM binding: some five hydrogens are not solvent accessible after binding at 25 min D_2O incubation time (Table 1). This can only be explained by changes in structure or protein dynamics upon ligand binding. The latter would be in agreement with the conformational equilibrium between two conformers of Syk tSH2 in the unbound form and the pronounced effect in protein-peptide binding affinity that restraining the relative position of the two SH2 domains may induce [19, 20]. Protein fragments L103-L123 and V132-L148, both participating in the inter-SH2 linker motif, undergo high deuterium incorporation (approximately 90%) as does the protein fragment R253-N269 (Table 1) in the ligand-free situation. The latter protein fragment, R253-N269,

lacks secondary structure, which leads us to hypothesize that the inter-SH2 domain region could exist in a random coil or low degree of secondary structure in the ligand-free protein, which turns into a higher helical structure in the ligand-bound form, as observed in the crystal structure of the Syk-ITAM complex (Figure 8). Consistent with our results, for the family-related Zap-70 kinase, only broad amide NMR signals could be detected for the two helices connecting the SH2 domains in the absence of the ITAM peptide. NMR and CD studies suggested a stabilization of helical structure for this region.

The Binding Site in the C-Terminal SH2 Domain

Each SH2 domain of Syk contains two binding pockets, which selectively bind a pYxxL/I motif of the ITAM peptide. In the crystal structure of Syk tSH2 in complex with ε -2pITAM, the peptide binds to the SH2 domain head-to-tail [17]; that is, the N-terminal pYxxL/I motif of the ITAM peptide binds the C-SH2 domain, whereas the C-terminal pYxxL/I binds the N-SH2 domain. The

Table 1. Deuterium uptake in protein segments after pepsin digestion

Peptide	Mass MH ⁺	N	Domain	pY _C /pY _N binding & SH2- SH2 interface	%D _{on} (ligand-free)	%D _{on} (ligand- bound)	D _{free} - D _{bound}
F17-E23	836.4266	7	Syk-N	R22(α A2), T21(α A1), E(α A3)	68	47	yes (1.5)
Y39-N46	1049.5856	8	Syk-N	R42(β B5), N46(BC2)	30	17	yes (1)
Y39-G50	1439.7759	12	Syk-N	R42(β B5), N46(BC2)	55	46	yes (1)
Y39-F51	1586.8443	13	Syk-N	R42(β B5), N46(BC2)	59	47	yes (1.5)
F51-E67	1937.0146	17	Syk-N	–	16	16	no
A52-E67	1789.9462	16	Syk-N	–	15	15	no
R68-Y74	852.4215	7	Syk-N	–	67	67	no
Y74-L88	1499.7606	14	Syk-N	–	52	40	yes (1.5)
A75-L88	1336.6973	13	Syk-N	–	52	38	yes (1.5)
L88-G98	1275.5064	11	Syk-N	–	–	–	–
L103-L123	2396.3090	17	Syk-N/Inter SH2	–	92	78	yes (2)
V132-L148	1940.0605	17	Inter SH2	–	92	62	yes (5)
I158-E176	2239.1446	18	Inter SH2/Syk-C	R175(α A2)	68	55	yes (2)
A159-I181	2712.3204	22	Inter SH2/Syk-C	R175(α A2)	70	59	yes (2.2)
I184-F192	951.5263	9	Syk-C	–	65	65	no
L193-S202	1115.5921	10	Syk-C	R195(β B5), R197(β B7)	33	23	yes (1)
L193-L205	1462.7766	13	Syk-C	R195(β B5), R197(β B7)	38	30	yes (1)
L205-F234	3465.9408	29	Syk-C	–	42	42	no
R253-N269	1826.9911	16	Syk-C	–	90	90	no

In column 1 and 2, the peptides analyzed and their corresponding masses are given. In column 3, N is the number of peptide amide protons in the peptide. In column 5, the protein amino acid residues with direct binding contacts with the phosphotyrosines (pY_C and pY_N) of the ITAM peptide, as well as the amino acid residues at the SH2-SH2 interface are given.[17] In the columns 6 and 7, the percentage of deuterium incorporation in the peptide either in the ligand-free or ligand-bound situation is given. In column 8, the difference in the number of deuteriums incorporated between the ligand-free and ligand-bound situation after 25 min incubation in buffered D₂O is shown.

mode of binding in each SH2 domain resembles closely that of the SH2 domains of the Src family of proteins, i.e., one pocket, positively charged, accommodates the phosphotyrosine, whereas the other, hydrophobic in nature, buries the nonpolar Ile/Leu residue at the +3 position C-terminal to the phosphotyrosine[50]. Two regions where exchange protection is observed lie in the binding site of Syk C-SH2 to the phosphotyrosine pY_NxxL of γ -2p-ITAM. The peptide fragments L193-S202 and L193-L205 comprise one region, and peptide fragments I158-E176 and A159-I181 encompass the second one. The phosphotyrosine binding side of Syk C-SH2 has, in the crystal structure [17, 51], several interactions with the bound ITAM peptide. Four arginine residues are in close proximity to the phosphotyrosine-binding site. Three of these residues, β B7 (R195), α A2 (R175), and β B5 (R197), contribute to the network of hydrogen bonds coordinating the phosphate group of the phosphotyrosyl residue. Arginine 175 (α A2) also makes a weak amino-aromatic interaction with the phosphotyrosine ring. Our data shows (Table 1) that in the region L193-S205, one hydrogen is protected in the ligand-bound form, and that in the region I158-I181, approximately two hydrogens are protected upon binding (Table 1).

The Binding Site in Syk N-SH2

Our data reveal that region Y39-F51 (peptides Y39-N46, Y39-G50, and Y39-F51) and F17-E23 are exchange-protected upon binding. Both regions lie in the binding site of Syk N-SH2 to the phosphotyrosine motif pYETL of γ -2pITAM. The C-terminal phosphotyrosine forms

hydrogen-bonding contacts with arginine residues α A2 (R22) and β B5 (R42) through its phosphate group [17]. Moreover, arginine α A2 (R22) makes a weak amino-aromatic interaction with the phenyl ring and a hydrogen bond with the carbonyl oxygen of pY_C-1. Leucine (pY_C+3) inserts deeply into the hydrophobic binding pocket of Syk N-SH2. Peptides Y74-L88 and A75-L88 encompass partly the hydrophobic binding pocket and are also found to be protected. The side-chain of isoleucine β E4 (I76), the carbon of the carbonyl group of Gly EF2 (G78), and the α carbon of Gly EF3 (G79) are between 3.9 and 4.3 Å from the side-chain of Ile pY_C+3.

The SH2-SH2 Interface

The nature of the amino acids located between the two phosphotyrosine binding motifs of the 2pITAM used in this study differs from the ones of the ε -2pITAM peptide used in the crystal structure. In the crystal structure, the pY linker only accounts for a small percentage of the total peptide surface buried upon binding; moreover, very few contacts are observed between the protein and peptide linker residues. Hence, the nature of the amino acids in the linker does not significantly affect binding, but its length could determine the restraint in movement imposed on the SH2 domains. The spacer length of the ε -2pITAM and that of the γ -2pITAM used in this study are alike, and therefore, the restraint imposed on the two SH2 domains and their SH2-SH2 interface should be similar. In the crystal structure, there are two main regions of inter-domain contacts: in the first region, the BC-loop in Syk N-SH2 faces the β F-strand, the FB-loop, and the N-terminal tip

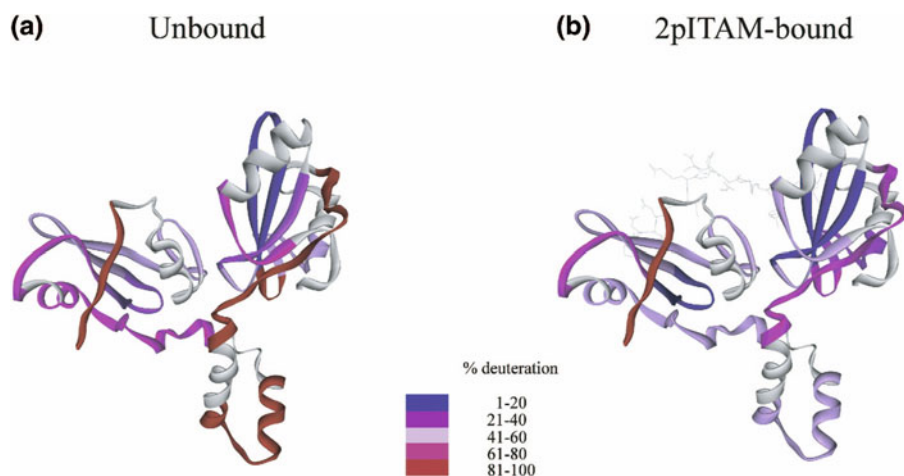


Figure 8. H/D exchange experimental results after 25 min incubation in buffered D₂O mapped onto the X-ray structure of Syk tSH2. (a) Ribbon diagrams depicting the percentage of deuterium incorporated in the different peptides probes in the case of the ligand-free Syk tSH2 and (b) the peptide ligand-bound Syk tSH2 with ITAM. The color codes range from red (81–100% deuterium incorporation) to blue (1–20% deuterium incorporation). Gray segments represent parts of the protein that could not be covered in the analysis. Note that in comparison with Figure 1 the structures are now rotated by 180 degrees.

of the α B helix of Syk C-SH2. Differences in deuterium exchange upon binding are observed in the BC loop of Syk N-SH2 (protein fragments Y39-N46, Y39-G50, and Y39-F51) (Table 1). These differences can be accounted for by the formation of both the SH2-SH2 interface as well as by direct contacts with the C-terminal phosphotyrosine of the ITAM peptide (see above). Unfortunately, no exchange kinetics could be followed for the protein fragments of the FB-loop or the α B helix of Syk C-SH2 (Figure 6). The second region of inter-domain contacts, the N-terminal end of the α A helix and the AA loop of Syk N-SH2, make contacts with residues in the C-terminal end of the α B helix of Syk C-SH2. As in the former interface region, peptide F17-E23 (Table 1) shows exchange protection, which could again be explained in terms of either SH2-SH2 interface or direct contacts with the ITAM peptide (see above).

To summarize, in Figure 8 the percentage of total exchangeable hydrogens exchanged after 25 min D₂O incubation are depicted for both the ligand-free (Figure 8a) and the bound Syk tSH2 (Figure 8b). Exchange protection upon binding in some regions of the SH2 domains can be readily explained in terms of peptide shielding: these regions are directly involved in the protein-peptide binding site(s). Although no structure of ligand-free Syk tSH2 is available to date, a good overview of the protein dynamics can be obtained from its family-related Zap-70 (Figure 1b) kinase. In the NMR and crystallographic study of the tSH2 domains of the latter protein [18], it is clearly shown that the almost complete length of the inter-SH2 domain is very dynamic. Similarly, in the Syk tSH2 protein (Figure 8a), the most solvent accessible regions (red) are encountered in the inter-SH2 linker region and C-terminus. The easily accessible protein fragments localized in the

inter-SH2 domain region undergo an extensive reduction in solvent accessibility upon ITAM binding (Figure 8b), which we propose is attributable to a dramatic increase in structural ordering or reduction in backbone dynamics by hydrogen bonding.

Conclusions

The relative orientation of the tandem SH2 domains of the Syk kinase seems to be very adaptable, similar to the tSH2 domains of its family partner Zap-70 kinase. Moreover, a highly flexible inter-SH2 domain linker region seems to play a key role in the overall dynamics of the protein. After ITAM binding, the tSH2 domains become locked into a more restricted conformation [19, 20]. By using H/D exchange in combination with enzymatic digestion and MALDI-TOF analysis, we probed not only the direct binding site of the ITAM peptide with Syk tSH2 but also the accompanying conformational effects in distal positions at the inter-SH2 domain at a medium structural resolution. The results show clearly that the overall inter-SH2 linker region becomes highly stabilized upon ITAM peptide binding. The conformational flexibility in Syk tSH2 matches with its functional ubiquity as Syk is a key mediator in a variety of signal transduction pathways. The conformational changes of the inter-SH2 domain linker region of Syk demonstrated in this report might be affected by conformational changes in other parts of the full Syk tyrosine kinase, namely, by the linker region between the tSH2 domain and the kinase domain or by the kinase domain itself. However, the indication that the SH2 domains of Syk seem to adopt a variety of relative orientations to accommodate diverse ligands [20], together with the stabilization that its inter-SH2 domain

linker undergoes upon ITAM binding, make it plausible that this conformational change(s) is one of the key signaling events involved in the activation of the kinase domain in Syk.

Acknowledgments

This article is in honor of Professor Michael T. Bowers, recipient of the 2004 ASMS Award for a Distinguished Contribution in Mass Spectrometry.

The authors thank the Utrecht Institute for Pharmaceutical Sciences (UIPS) for financial support and Dr. Nico de Mol, Department of Medicinal Chemistry, Utrecht University, for stimulating discussions.

References

- Turner, M.; Schweighoffer, E.; Colucci, F.; Di Santo, J. P.; Tybulewicz, V. L. Tyrosine kinase SYK: Essential Functions for Immunoreceptor Signaling. *Immunol. Today* **2000**, *21*, 148–154.
- Yanagi, S.; Inatome, R.; Takano, T.; Yamamura, H. Syk Expression and Novel Function in a Wide Variety of Tissues. *Biochem. Biophys. Res. Commun.* **2001**, *288*, 495–498.
- Reth, M. Antigen Receptor Tail Clue. *Nature* **1989**, *338*, 383–384.
- Pribluda, V. S.; Pribluda, C.; Metzger, H. Transphosphorylation as the Mechanism by Which the High-Affinity Receptor for IgE is Phosphorylated Upon Aggregation. *Proc. Natl. Acad. Sci. U.S.A.* **1994**, *91*, 11246–11250.
- Cambier, J. C.; Pleiman, C. M.; Clark, M. R. Signal Transduction by the B Cell Antigen Receptor and Its Coreceptors. *Annu. Rev. Immunol.* **1994**, *12*, 457–486.
- Chan, A. C.; Desai, D. M.; Weiss, A. The Role of Protein Tyrosine Kinases and Protein Tyrosine Phosphatases in T Cell Antigen Receptor Signal Transduction. *Annu. Rev. Immunol.* **1994**, *12*, 555–592.
- Kimura, T.; Sakamoto, H.; Appella, E.; Siraganian, R. Conformational Changes Induced in the Protein Tyrosine Kinase p72syk by Tyrosine Phosphorylation or by Binding of Phosphorylated Immunoreceptor Tyrosine-Based Activation Motif Peptides. *Mol. Cell. Biol.* **1996**, *16*, 1471–1478.
- Shiue, L.; Zoller, M. J.; Brugge, J. S. Syk is Activated by Phosphotyrosine-Containing Peptides Representing the Tyrosine-Based Activation Motifs of the High Affinity Receptor for IgE. *J. Biol. Chem.* **1995**, *270*, 10498–10502.
- Hatada, M. H.; Lu, X. D.; Laird, E. R.; Green, J. P.; et al. Molecular Basis for Interaction of the Protein Tyrosine Kinase ZAP-70 with the T-Cell Receptor. *Nature* **1995**, *377*, 32–38.
- Sada, K.; Zhang, J.; Siraganian, R. P. SH2 Domain-Mediated Targeting, but not Localization, of Syk in the Plasma Membrane is Critical for Fc[epsilon]RI Signaling. *Blood* **2001**, *97*, 1352–1359.
- Sicheri, F.; Moarefi, I.; Kuriyan, J. Crystal Structure of the Src Family Tyrosine Kinase Hck. *Nature* **1997**, *385*, 602–609.
- Arold, S. T.; Ulmer, T. S.; Mulhern, T. D.; Werner, J. M.; Ladbury, J. E.; Campbell, I. D.; Noble, M. E. M. The Role of the Src Homology 3-Src Homology 2 Interface in the Regulation of Src Kinases. *J. Biol. Chem.* **2001**, *276*, 17199–17205.
- Engh, R. A.; Bossemeyer, D. Structural Aspects of Protein Kinase Control—Role of Conformational Flexibility. *Pharmacol. Ther.* **2002**, *93*, 99–111.
- Grucza, R.; Bradshaw, J.; Mitaxov, V.; Waksman, G. Role of Electrostatic Interactions in SH2 Domain Recognition: Salt Dependence of Tyrosyl-Phosphorylated Peptide Binding to the Tandem SH2 Domain of the Syk Kinase and the Single SH2 Domain of the Src Kinase. *Biochemistry* **2000**, *39*, 10072–10081.
- Dekker, F. J.; de Mol, N. J.; van Ameijde, J.; Fischer, M. J. E.; Ruijtenbeek, R.; Redegeld, F. A. M.; Liskamp, R. M. J. Replacement of the Intervening Amino Acid Sequence of a Syk-Binding Diphosphopeptide by a Nonpeptide Spacer with Preservation of High Affinity. *Chem. Biochem.* **2002**, *3*, 238–242.
- Dekker, F. J.; de Mol, N. J.; Fischer, M. J.; Liskamp, R. M. Amino Propynyl Benzoic Acid Building Block in Rigid Spacers of Divalent Ligands Binding to the Syk SH2 Domains with Equally High Affinity as the Natural Ligand. *Bioorg. Med. Chem. Lett.* **2003**, *13*, 1241–1234.
- Fütterer, K.; Wong, J.; Grucza, R. A.; Chan, A. C.; Waksman, G. Structural Basis for Syk Tyrosine Kinase Ubiquity in Signal Transduction Pathways Revealed by the Crystal Structure of Its Regulatory SH2 Domains Bound to a Dually Phosphorylated ITAM Peptide 1. *J. Mol. Biol.* **1998**, *281*, 523–537.
- Folmer, R. H. A.; Geschwindner, S.; Yafeng Xue, Y. Crystal Structure and NMR Studies of the Apo SH2 Domains of ZAP-70: Two Bikes Rather than a Tandem. *Biochemistry* **2002**, *41*, 14176–14184.
- Grucza, R. A.; Fütterer, K.; Chan, A. C.; Waksman, G. Thermodynamic Study of the Binding of the Tandem-SH2 Domain of the Syk Kinase to a Dually Phosphorylated ITAM Peptide: Evidence for Two Conformers. *Biochemistry* **1999**, *38*, 5024–5033.
- Kumaran, S.; Grucza, R. A.; Waksman, G. The Tandem Src Homology 2 Domain of the Syk Kinase: A Molecular Device that Adapts to Interphosphotyrosine Distances. *Proc. Natl. Acad. Sci. U.S.A.* **2003**, *100*, 14828–14833.
- Anderegg, R.; Wagner, D. Mass Spectrometric Characterization of Protein–Ligand Interaction. *J. Am. Chem. Soc.* **1995**, *117*, 1374–1377.
- Guy, P.; Remigy, H.; Jaquinod, M.; Bersch, B.; Blanchard, L.; Dolla, A.; Forest, E. Study of the New Stability Properties Induced by Amino Acid Replacement of Tyrosine 64 in Cytochrome c553 from *Desulfovibrio vulgaris* Hildenborough Using Electrospray Ionization Mass Spectrometry. *Biochem. Biophys. Res. Commun.* **1996**, *218*, 97–103.
- Zhang, Z.; Smith, D. L. Determination of Amide Hydrogen Exchange by Mass Spectrometry: A New Tool for Protein Structure Elucidation. *Protein Sci.* **1993**, *2*, 522–531.
- Mandell, J. G.; Falick, A. M.; Komives, E. A. Measurement of Amide Hydrogen Exchange by MALDI-TOF Mass Spectrometry. *Anal. Chem.* **1998**, *70*, 3987–3995.
- Catalina, M. I.; Dekker, F. J.; Liskamp, R. M. J.; Versluis, C.; Maier, C. S.; Heck, A. J. R. Structural Analysis of High Affinity Divalent Phosphopeptide Hybrids of Spleen Tyrosine Kinase. *Int. J. Mass Spectrom.* **2003**, *228*, 879–890.
- de Mol, N. J.; Catalina, M. I.; Fischer, M. J. E.; Broutin, I.; Maier, C. S.; Heck, A. J. R. Changes in Structural Dynamics of the Grb2 Adaptor Protein Upon Binding of Phosphotyrosine Ligand to Its SH2 Domain. *Biochem. Biophys. Acta* **2004**, *1700*, 53–64.
- Kipping, M.; Schierhorn, A. Improving Hydrogen/Deuterium Exchange Mass Spectrometry by Reduction of the Back-Exchange Effect. *J. Mass Spectrom.* **2003**, *38*, 271–276.
- Thevenon-Emeric, G.; Kozlowski, J.; Zhang, Z.; Smith, D. L. Determination of Amide Hydrogen Exchange Rates in Peptides by Mass Spectrometry. *Anal. Chem.* **1992**, *64*, 2456–2458.
- Jensen, O. A.; Podtelejnikov, A.; Mann, M. Delayed Extraction Improves Specificity in Database Searches by Matrix-Assisted Laser Desorption/Ionization Peptide Maps. *Rapid Commun. Mass Spectrom.* **1996**, *10*, 1371–1378.
- Zhang, Z.; Smith, D. L. Determination of Amide Hydrogen Exchange by Mass Spectrometry: A New Tool for Protein Structure Elucidation. *Protein Sci.* **1993**, *2*, 522–531.

31. Dharmasiri, K.; Smith, D. L. Mass Spectrometric Determination of Isotopic Exchange Rates of Amide Hydrogens Located on the Surfaces of Proteins. *Anal. Chem.* **1996**, *68*, 2340–2344.
32. Yan, X.; Broderick, D.; Leid, M.; Schimerlik, M.; Deinzer, M. Dynamics and Ligand-Induced Solvent Accessibility Changes in Human Retinoid X Receptor Homodimer Determined by Hydrogen Deuterium Exchange and Mass Spectrometry. *Biochemistry* **2004**, *43*, 909–917.
33. Yan, X.; Watson, J.; Ho, P. S.; Deinzer, M. L. Mass Spectrometric Approaches Using Electrospray Ionization Charge States and Hydrogen–Deuterium Exchange for Determining Protein Structures and Their Conformational Changes. *Mol. Cell. Proteom.* **2004**, *3*, 10–23.
34. Miranker, A.; Robinson, C. V.; Radford, S. E.; Aplin, R. T.; Dobson, C. M. Detection of Transient Protein Folding Populations by Mass Spectrometry. *Science* **1993**, *262*, 896–900.
35. Wagner, D. S.; Melton, L. G.; Yan, Y.; Erickson, B. W.; Anderegg, R. J. Deuterium Exchange of α -Helices and β -Sheets as Monitored by Electrospray Ionization Mass Spectrometry. *Protein Sci.* **1994**, *3*, 1305–1314.
36. Mandell, J. G.; Baerga-Ortiz, A.; Akashi, S.; Takio, K.; Komives, E. A. Solvent Accessibility of the Thrombin–Thrombomodulin Interface. *J. Mol. Biol.* **2001**, *306*, 575–589.
37. Wintrode, P.; Friedrich, K.; Vierling, E.; Smith, J.; Smith, D. Solution Structure and Dynamics of a Heat Shock Protein Assembly Probed by Hydrogen Exchange and Mass Spectrometry. *Biochemistry* **2003**, *42*, 10667–10673.
38. Croy, C.; Koeppe, J.; Bergqvist, S.; Komives, E. Allosteric Changes in Solvent Accessibility Observed in Thrombin Upon Active Site Occupation. *Biochemistry* **2004**, *43*, 5246–5255.
39. Andersen, M. D.; Shaffer, J.; Jennings, P. A.; Adams, J. A. Structural Characterization of Protein Kinase A as a Function of Nucleotide Binding. Hydrogen–Deuterium Exchange Studies Using Matrix-Assisted Laser Desorption Ionization–Time of Flight Mass Spectrometry Detection. *J. Biol. Chem.* **2001**, *276*, 14204–14211.
40. Dekker, F. J.; de Mol, N. J.; Fischer, M. J. E.; Liskamp, R. M. J. Amino Propynyl Benzoic Acid Building Block in Rigid Spacers of Divalent Ligands Binding to the Syk SH2 Domains with Equally High Affinity as the Natural Ligand. *Bioorg. Med. Chem. Lett.* **2003**, *13*, 1241–1244.
41. Hvidt, A.; Linderstrom-Lang, K. Exchange of Hydrogen Atoms in Insulin with Deuterium Atoms in Aqueous Solutions. *Biochem. Biophys. Acta* **1954**, *14*, 575–575.
42. Hoofnagle, A. N.; Resing, K. A.; Ahn, N. G. Protein Analysis by Hydrogen Exchange Mass Spectrometry. *Annu. Rev. Biophys. Biomol. Struct.* **2003**, *32*, 1–25.
43. Engen, J. R.; Gmeiner, W. H.; Smithgall, T. E.; Smith, D. L. Hydrogen Exchange Shows Peptide Binding Stabilizes Motions in Hck SH2. *Biochemistry* **1999**, *38*, 8926–8935.
44. Farrow, N. A.; Muhandiram, R.; Singer, A. U.; Pascal, S. M.; Kay, C. M.; Gish, G.; Shoelson, S. E.; Pawson, T.; Forman-Kay, J. D.; Kay, L. E. Backbone Dynamics of a Free and Phosphopeptide-Complexed Src Homology 2 Domain Studied by ^{15}N NMR Relaxation. *Biochemistry* **1994**, *33*, 5984–6003.
45. Shoelson, S. E.; Sivaraja, M.; Williams, K. P.; Hu, P.; Schlessinger, J.; Weiss, M. A. Specific Phosphopeptide Binding Regulates a Conformational Change in the PI 3-Kinase SH2 Domain Associated with Enzyme Activation. *Embo J.* **1993**, *12*, 795–802.
46. Breeze, A. L.; Kara, B. V.; Barratt, D. G.; Anderson, M.; Smith, J. C.; Luke, R. W.; Best, J. R.; Cartledge, S. A. Structure of a Specific Peptide Complex of the Carboxy-Terminal Sh2 Domain from the P85- α Subunit of Phosphatidylinositol 3-Kinase. *Embo J.* **1996**, *15*, 3579–3589.
47. Van den Bremer, E. T. J.; Jiskoot, W.; James, R.; Moore, G. R.; Kleanthous, C.; Heck, A. J. R.; Maier, C. S. Probing Metal Ion Binding and Conformational Properties of the Colicin E9 Endonuclease by Electrospray Ionization Time-of-Flight Mass Spectrometry. *Protein Sci.* **2002**, *11*, 1738–1752.
48. Mohimen, A.; Dobo, A.; Hoerner, J. K.; Kaltashov, I. A. A Chemometric Approach to Detection and Characterization of Multiple Protein Conformers in Solution Using Electrospray Ionization Mass Spectrometry. *Anal. Chem.* **2003**, *75*, 4139–4147.
49. Konermann, L.; Douglas, D. J. Equilibrium Unfolding of Proteins Monitored by Electrospray Ionization Mass Spectrometry: Distinguishing Two-State from Multi-State Transitions. *Rapid Commun. Mass Spectrom.* **1998**, *12*, 435–442.
50. Waksman, G.; Shoelson, S. E.; Pant, N.; Cowburn, D.; Kuriyan, J. Binding of a High Affinity Phosphotyrosyl Peptide to the Src SH2 Domain: Crystal Structures of the Complexed and Peptide-Free Forms. *Cell* **1993**, *72*, 779–790.
51. Narula, S.; Yuan, R.; Adams, S.; Green, O.; Green, J.; Philips, T.; Zydowsky, L.; Botfield, M.; Hatada, M.; Laird, E.; Zoller, M.; Karas, J.; Dalgarno, D. Solution Structure of the C-Terminal SH2 Domain of the Human Tyrosine Kinase Syk Complexed with a Phosphotyrosine Pentapeptide. *Structure* **1995**, *3*, 1061–1073.